Canadian Conference - Pacific Conference on Earthquake Engineering 2023

Vancouver, British Columbia

June 25th – June 30th, 2023

Suitability of Frames with Intentionally Eccentric Braces as the Seismic-Force-Resisting System of High-Rise Buildings

Andrés González Ureña[1*], Robert Tremblay[2] and Colin A. Rogers[3]

[1]Professor, School of Civil Engineering and Earthquake Engineering Laboratory, Universidad de Costa Rica, San José, Costa Rica
[2]Professor, Department of Civil, Geological and Mining Engineering, Polytechnique Montréal, Montréal, QC, Canada
[3]Professor, Department of Civil Engineering, McGill University, Montréal, QC, Canada
[*]andres.gonzalezurena@ucr.ac.cr (Corresponding Author)

ABSTRACT

The Frame with Intentionally Eccentric Braces (FIEB) is a novel seismic-force-resisting system (SFRS) that overcomes several of the limitations of the widely adopted Concentrically Braced Frame (CBF), namely those related to its high elastic stiffness and marginal inelastic stiffness. Recent numerical studies have shown that, in comparison to equivalent CBFs, low- and mid-rise FIEBs offer an improved structural response to earthquake loading at a reduced cost owing to their significant post-elastic stiffness and to the better control over the overstrength.

Another presumed advantage of FIEBs is that the stability of tall buildings under seismic action could be ensured through design by selecting the eccentric braces so that their post-elastic stiffness at each storey at the expected displacement is greater than the negative geometric stiffness, thus preventing the overshooting of storey drift demands due to the P-Δ effects. Moreover, the fact that a portion of the cross-section of the bracing members remains in the elastic range as they engage in plastic energy dissipation provides the frame with partial self-centering capability, further enhancing its stability.

In this article, the suitability of FIEBs as the SFRS of high-rise buildings is investigated. 40-, 30-, and 20-storey model buildings, located in Vancouver, BC, are designed employing a revision of a displacement-based design procedure previously developed by the authors, and their seismic performance is assessed numerically through Non-Linear Response History Analysis (NLRHA). The results show that the so designed FIEBs exhibit a satisfactory response to ground motions, including those from long duration subduction earthquakes, suggesting that the FIEB system is indeed adequate for use in high-rise buildings.

Keywords: FIEBs, BIEs, steel braces, earthquake-resistant design, Non-Linear Response History Analysis.

INTRODUCTION

Braces with Intentional Eccentricity (BIEs) have been proposed as an alternative to traditional Concentrically Loaded Braces (CLBs) offering an improved structural performance [1]. Because of the offset between the bracing member's axis and the working points' axis, axial force in BIEs is accompanied by flexure. As such, the elastic stiffness of a BIE is inversely proportional to the eccentricity and inherently lower than that of a CLB of the same cross-section. Also, once the yielding stress is attained in the extreme fibre, plasticity progresses gradually through the cross-section, resulting in significant post-elastic stiffness, in contrast with the very low plastic stiffness of a CLB for which the entire cross-section yields instantaneously under pure axial load. A comprehensive description of the response of BIEs to monotonic and cyclic loading and of the influence of the variables involved can be found in [2] and [3].

When employed in Frames with Intentionally Eccentric Braces (FIEBs), these characteristics of BIEs translate to several advantages in comparison to Concentrically Braced Frames (CBFs). The lower stiffness of BIEs results in structures with higher fundamental periods, which are thus subjected to lower spectral accelerations and seismic design forces. Additionally, the possibility of adjusting through the prescribed eccentricity the elastic and post-elastic stiffness of each storey allows for a greater control of the dynamic response of the structure and for a reduction of incidental overstrength. Together, these features help to reduce the overall cost of the structure, especially when capacity-based design forces are considered, and render FIEBs well suited to performance-oriented design, as the compliance with performance objectives associated with different levels of seismic hazard can easily be ensured in design [3-5].

Another purported benefit of FIEBs is that the substantial post-elastic stiffness of the BIEs would allow their use in high-rise buildings, as it could ensure the stability of the structure by counteracting the P-Δ effects. That is, by selecting at each storey braces that offer a minimum lateral stiffness larger than the negative geometric stiffness, excursion of the structure beyond the stable equilibrium point could presumably be prevented. Given the difficulty in controlling large inelastic storey drift demands due to their limited post-yielding stiffness and the associated risk of instability, particularly in the case of long subduction ground motions, most modern design codes limit the maximum height of CBFs. For example, CSA S16-19 allows moderately ductile (MD) and limited-ductility (LD) CBFs in seismic categories SC3 and SC4 up to 40 m and 60 m in height, respectively [6].

The suitability of FIEBs with rectangular HSS BIEs as the SFRS of high-rise buildings is explored in this article. To this effect, 20-, 30-, and 40-storey model buildings are designed for the seismic hazard of downtown Vancouver, BC, using a revision of the design procedure described in [4] and their response to earthquake loading is then assessed numerically through Non-Linear Response History analysis (NLRHA) performed in OpenSees [7].

REVISIONS TO THE DESIGN PROCEDURE

The procedure employed herein for the design of high-rise FIEB buildings is a revision of the procedure first presented by the authors in [3], and subsequently refined to include performance objectives for service-level earthquake demands in [4]. It is based on the Direct Displacement-Based Design methodology as introduced by Priestley et al. [8]. Considering that the force that BIEs develop depends directly on the imposed displacement, and that the theoretical capacity of the bracing member section is attained at displacements far greater than the permissible storey drift ratios, the traditional force-based design method was deemed incompatible with FIEBs and, thus, a displacement-based approach was selected. In the following paragraphs, the changes implemented in the design procedure with respect to the previous version, which is described thoroughly in [3] and [4], are discussed.

Simplified design backbone curves

Previously, the force-displacement design parameters of BIEs employed in design were obtained independently for braces in tension and in compression. For braces in tension, the resulting force-displacement curves under monotonic loading of fibre-based numerical models of BIEs with nominal material strength in OpenSees were simplified to bi-linear backbone curves, defined by the first-yield and ultimate-yield points. For braces in compression, an elastic-perfectly plastic curve was adopted, with the maximum load taken as equal to the calculated critical load of the BIE idealized as a column under eccentric loading. Together, these two curves would furnish all the relevant properties of the BIEs' response for design effects, i.e., estimating the force that the pair of BIEs acting in tandem would develop as a function of the storey displacement. Although this approach produced satisfactory outcomes in the design of FIEBs up to 12 storeys in height, some adjustments were enacted in this study to better estimate the effective stiffness provided by the pair of BIEs.

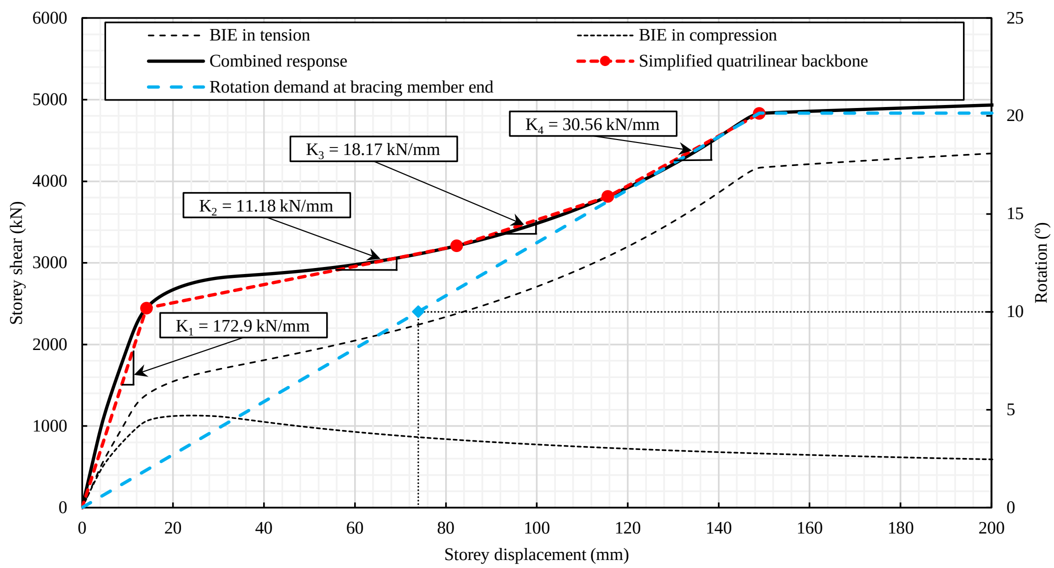

Figure 1. Example of the response of a BIE pair under monotonic loading and simplified backbone curve.

Simplified backbone curves based on the monotonic response of numerical models of BIEs in tension and in compression are still used, but these are now based on the combined response of the two braces in terms of storey shear (lateral force) vs. displacement. Additionally, the revised simplified backbone is quatri-linear, in lieu of bi-linear, to better match the effective lateral stiffness of the BIE pair as the displacement increases. The points that define this curve are the estimated first-yield point (δ_y, v_y), the ultimate-yield point (δ_u, v_u), and, between those, the points with displacements equal to $\frac{1}{2}(\delta_u - \delta_y)$ and $\frac{3}{4}(\delta_u - \delta_y)$. Thus, the backbone curve is composed of 4 segments with stiffnesses K_1 to K_4. Typically, K_2 is the minimum storey shear stiffness that a given pair of BIEs provides. The combined numerical response and backbone curves of a pair of CSA G40.21-350W HSS 254×254×16 BIEs with an eccentricity of 250 mm designed for 6 m by 4 m braced bents are presented in Figure 1.

Minimum stiffness for control of P-Δ effects

In the previous version of the design procedure P-Δ effects were addressed by augmenting the design shears at each storey by the U_2 factor, as allowed by CSA S16 when a static analysis is used. While the use of the U_2 factor produces adequate results in most applications as it aims to ensure that the structure will dispose of sufficient strength to face the increment in force demand due to stability effects, it does not address explicitly the possibility of collapse due to large displacement demands when the effective lateral stiffness of a storey is negative. As such, in the design of tall buildings, for which the P-Δ effects are substantial and the spectral displacement demands are large due to their high fundamental period, the U_2 factor can fail to guarantee the structure's stability, especially if the seismic hazard comprises long duration subduction earthquakes. Therefore, to prevent the risk of collapse due to structural instability, the design procedure requires that the BIEs at each storey be selected so that the minimum storey shear stiffness, $K_{2,i}$, be always larger than the negative geometric stiffness of that storey (Eq. (1)), hence ensuring a strictly positive effective stiffness. $\Sigma C_{f,i}$ are the cumulated factored gravity loads affecting the ith storey and h its height.

$$K_{2,i} \geq \frac{\Sigma C_{f,i}}{h_i} \tag{1}$$

Prevention of fracture at bracing member's end

Experimental results [1, 2] have shown that BIEs under cyclic loading exhibit two possible failure modes: low-cycle-fatigue-induced fracture at the mid-length plastic hinge region after the onset of local buckling, the characteristic failure mode of CLBs as well, and fracture in tension at the bracing member's end. Photographs of both types of fracture are shown in Figure 2.

Figure 2. Failure modes of BIEs: low-cycle-fatigue-induce fracture (left) and tension fracture (right) (reproduced from [2]).

In terms of displacement demand, the onset of local buckling and subsequent low-cycle-fatigue-induced fracture is delayed in BIEs with respect to CLBs due to a more even distribution of the strain demands along the length of the brace as an effect of the eccentricity-induced flexural response. In general, the more compact the cross-section and the greater the eccentricity, the larger the displacement demands under cyclic loading that a BIE can safely sustain before developing plastic local buckling at mid-length. The authors proposed an equation that estimates the allowable design drift ratio as per this criterion for square HSS

BIEs as a function of the eccentricity to section height ratio, e/H, and a combined global and local slenderness parameter $(L/r)/(b_{el}/t)$ [9].

Fracture in tension at the bracing member's end is related to the concentration of strain demands in the region where the bracing member connects to the *eccentering* assembly (i.e., the component of BIEs that accommodates the eccentricity and links rigidly the brace proper to its connection to the frame). In theory, for the BIE to develop its tensile strength, $F_y A_g$, the effective eccentricity along its length must be annulled. This would require that the bracing member's ends develop the plastic rotation given by Eq. (2), θ_e, as described in [2]. In Eq. (2), L_{ea} is the length of the *eccentering* assembly and L_k is the effective hinging length of the connection plate.

$$\theta_e = \tan^{-1}\left(\frac{e}{L_{ea} + \frac{H + L_k}{2}}\right) \tag{2}$$

Given the limited available information on the rotation capacity of HSS members under tensile load, based on the experimental and numerical results presented in [2] it is estimated that BIEs under monotonic tension can sustain rotations at the bracing member's ends up to 10º, approximately. The results also show that the rotation at those regions is a linear function of the imposed displacement, thus the displacement at which the 10º rotation is attained can be estimated knowing the ultimate yield point displacement, δ_u. For example, for the BIEs whose response and idealized backbone curves are shown in Figure 1, the 10º rotation is attained at a lateral storey displacement close to 73 mm, equivalent to a storey drift of 1.8%.

Under cyclic or earthquake loading, however, the storey displacement at which a rotation of 10º at the bracing member's end is attained is significantly larger, since once the elastic range has been surpassed the imposed displacements in tension first rectify the deformations from the compression excursions before producing effective tension deformations. As the results in [2] show, the displacement at which BIEs attain a rotation of 10º at their bracing member's ends under cyclic loading is up to 77% larger than the corresponding displacement under monotonic tension load. Therefore, in this study the maximum allowable design drift ratio for BIEs is taken conservatively as the smaller between 1.5 times the drift associated with the displacement that produces a rotation of 10º at the bracing member's ends under monotonic tension loading, and the drift ratio calculated with the equation derived in [9].

Partial self-centering capability

In BIEs in the post-elastic stage a part of the cross-section remains in the elastic range as the compressive normal stresses due to bending counteract the tensile stresses associated with the axial load. Supposing that plasticization of the cross-section progresses as a linear function of the imposed displacement between the points corresponding to first-yield, δ_y, and ultimate-yield, δ_u, 25% of the cross-section of the BIE persists in the elastic range at a displacement equal to $\frac{3}{4}(\delta_u - \delta_y)$. This elastic portion of the BIE helps in reversing the deformations and displacements produced by the earthquake demands and, in doing so, reduces the permanent drift-ratios and contributes to enhance the overall stability of the structure. As such, an additional criterion in the selection of the BIEs in this study is that, for the pair of braces and their *eccentering* assemblies chosen for each storey, $\frac{3}{4}(\delta_u - \delta_y)$ be larger than the target displacement level to ensure partial self-centering capability.

SEISMIC PERFORMANCE OF HIGH-RISE FIEBs

The suitability of FIEBs designed as the SFRS of high-rise buildings, with the above-described design procedure, was evaluated for three buildings of consistent floor plan extending 20, 30, and 40 storeys in height, and assessing their performance through NLRHA. Downtown Vancouver, B.C., (49.25ºN, 123.12ºW) was selected as the location for the buildings on account of its high seismic hazard, including long duration subduction earthquakes which presumably govern the response of tall FIEBs. The site was assumed to have a mean shear wave velocity of 360 m/s (i.e., site designation X_{360}) and the seismic hazard design values were obtained from the online 2020 National Building Code of Canada Seismic Hazard Tool [10]. The plan configuration of the buildings and the gravity loads considered in their design are shown in Figure 3. The typical arrangement of the braced bents and a detail of the considered *eccentering* assembly are presented in Figure 4 and Figure 5, respectively. These are consistent with those employed in [2] and [3], and were selected for their simplicity and constructive efficiency, and to produce in-plane bending of the BIEs. The uniform storey height is 4 m.

Although one of the advantages of a displacement-based design procedure is that it allows in theory to select a target displacement, in practice the minimum stiffness condition and other requirements described in the previous section determine the maximum displacement objective that can be selected for high-rise BIEs while complying with all the proposed criteria. As such, the buildings in this study were designed for the maximum target drift ratio that the design procedure would concede for each building, in an effort to produce the most cost-effective solution. In each building, a single HSS size was employed for the BIEs, with their eccentricity increasing over the height. The maximum allowable eccentricity for the given HSS, complying with the stability criteria and all requirements of the design procedure, was selected at each storey. Despite the fact that it was verified that wind loading would govern the design of the lateral resistance system of the buildings, it was deliberately not considered in the design, as the intent was to study the outcome of the seismic design procedure. In Table 1, the target drift ratios of the buildings are presented, along with the resulting steel quantities for the SFRS (BIEs, columns, and beams), the HSS selected for the BIEs, the minimum and maximum eccentricities, and the periods of the first three vibration modes and their cumulative modal mass participation ratios (MMPR).

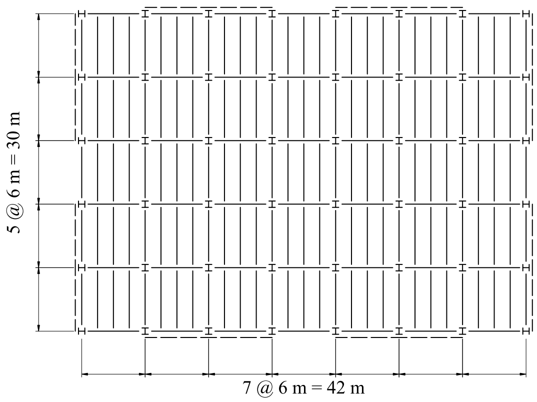

Gravity loads:		
Roof:	Dead = 1.35 kPa	
	Live = 1.0 kPa	
	Snow = 1.8 kPa	
Floors:	Dead = 3.6 kPa (+ 1.0 kPa partitions)	
	Live = 2.4 kPa	
Exterior walls:	Dead = 1.5 kPa	

Figure 3. Plan configuration of the buildings and design gravity loads.

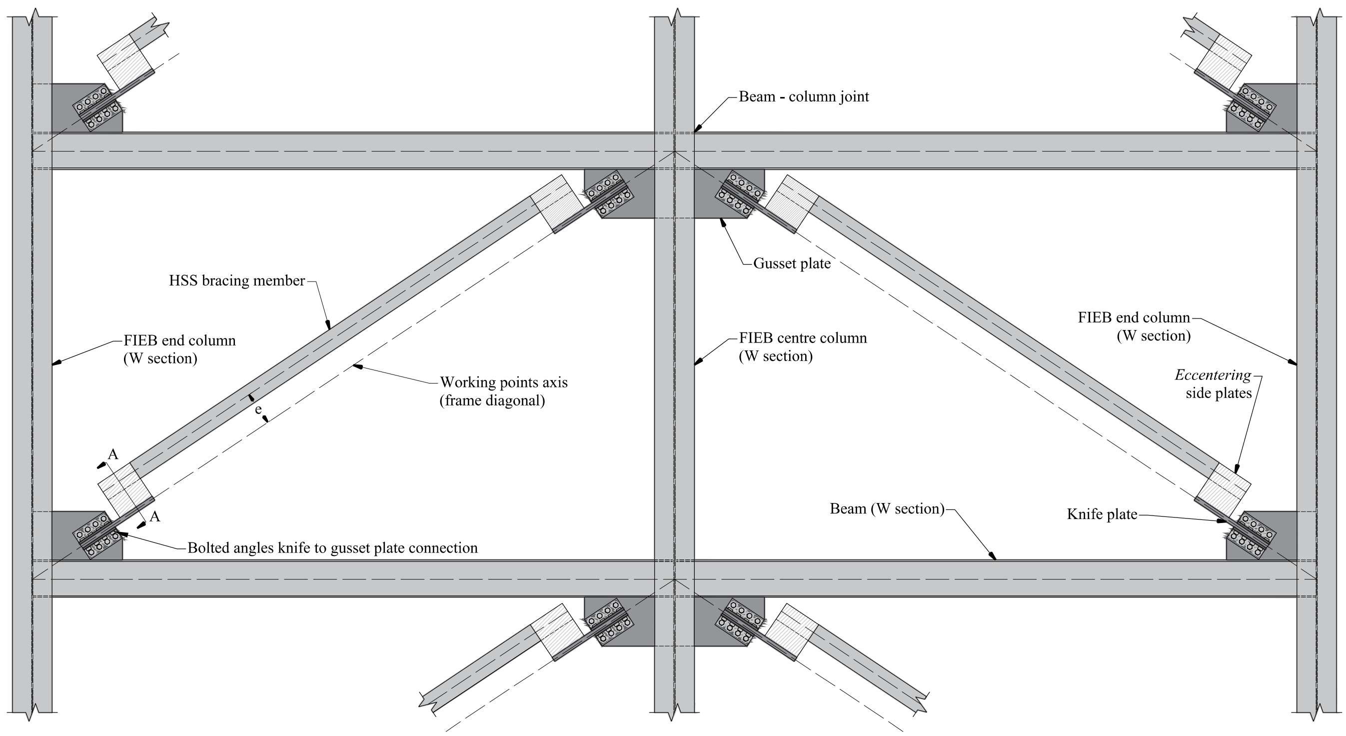

Figure 4. Typical arrangement of the braced bents.

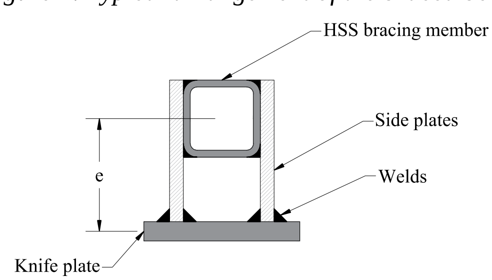

Figure 5. Detail of eccentering assembly (Section A-A of Figure 4).

Table 1. Design parameters and resulting properties of designed FIEBs.

FIEB	**Design drift ratio**	**SFRS tonnage**	**BIE HSS**	**Eccentricity range (mm)**	**1st mode**		**2nd mode**		**3rd mode**	
					T(s)	**MMPR**	**T(s)**	**MMPR**	**T(s)**	**MMPR**
40-storey	1.80%	494	254×254×16	180 – 460	7.44	0.636	2.39	0.837	1.30	0.902
30-storey	2.10%	273	254×254×16	220 – 460	5.53	0.667	1.85	0.857	1.02	0.915
20-storey	2.15%	104	178×178×16	200 – 360	4.32	0.704	1.51	0.878	0.85	0.929

Non-Linear Response History Analysis

To carry out the performance assessment, plane models of the designed FIEBs were programmed in OpenSees using fibre-based sections for the BIEs, beams, and columns. The *eccentering* assemblies and the hinging portion of the knife-plates connection of the BIEs were explicitly modelled with fibre-based sections while the remainder of the connection was introduced as a rigid link. The mass of each storey was lumped in the central node and diaphragm constraints were assigned. The P-Δ effects were incorporated in the models by employing a leaning column attached to the SFRS, to which the concomitant tributary gravity loads were applied. Rayleigh damping of 3% critical was specified, and the applied gravity loads were those corresponding to load combination 1.0 D + 1.0 E +0.5 L + 0.25 S.

Upper-bound yield strength values were used to model all members of the structure for determining both forces and displacement demands. It was verified that this resulted in maximum demand for both parameters and therefore represents the most severe scenario. In BIEs, the post-elastic stiffness increases with the yield stress and, thus, if the FIEB is modelled with a higher yield stress, its effective post-elastic period decreases and the structure is subjected to overall higher spectral acceleration demands throughout the analysis, resulting in larger displacements. As such, a yield stress of 1.2 times R_yF_y was considered for the steel materials in the models as per [11].

The ground motions employed in the NLRHA were selected and scaled in accordance with the guidelines of [11]. Two scenario-specific ground motion suites were employed to reflect the seismic hazard deaggregation for Vancouver described in [12]: one comprising 11 ground motions from crustal and in-slab subduction earthquakes, scaled to cover the period range from 0.60 s to 1.0 s, and another composed of 11 ground motions from interface subduction earthquakes for the period range from 1.0 to 10.0 s. A shortcoming of the employed ground motions is that the target period range should have spanned up to twice the fundamental period of the 40-storey FIEB, approximately 15 s, however there is no information available on the seismic hazard for periods larger than 10 s. The response spectra of the considered ground motions are shown in Figure 6. Only horizontal acceleration was considered.

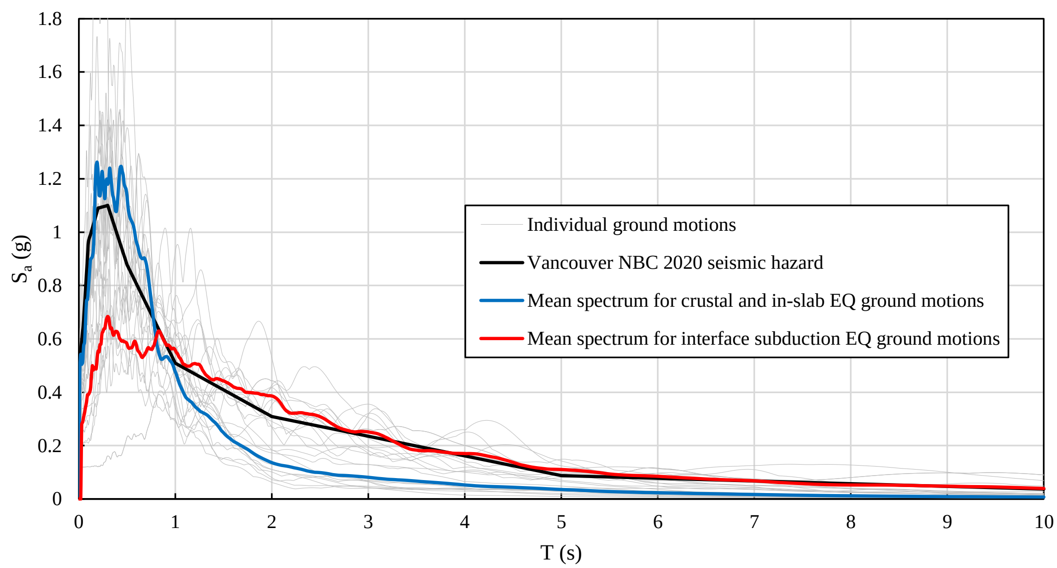

Figure 6. Mean response spectra of the ground motion suites used in the analyses.

Results

The maximum storey drifts obtained from the analyses of the three buildings are presented in Figure 7. No collapses nor extreme drift demand concentrations in particular storeys were observed, which reflects the design procedure's efficacy in maintaining stability by controlling the P-Δ effects. As expected, the interface subduction earthquake ground motions produce the largest drifts in all cases. The largest drift demands occur in the upper third of the buildings, with the contrast between lower and higher storeys being more marked as the building height increases. This behaviour is due to the higher mode effects, whose relative weight in the building's response increases with its height. For example, as given in Table 1, the first mode mass participation ratio varies from 0.704 for the 20-storey building to 0.636 for the 40-storey building.

In the case of the 20-storey building, the average maximum drift ratios are lower than the target drift ratio, indicated by the dotted lines in Figure 7. For the 30-storey building the average maximum storey drift ratios for the subduction earthquake ground motions exceed slightly the target drift ratio in 4 storeys but stay below the allowable limit of 2.5% [10], indicated by the dashed line. For the 40-storey building, the average maximum drift ratios exceed the target in storeys 27 through 39 and very narrowly surpass the 2.5% limit in three storeys. Except for one of the interface subduction ground motions in the case of the 40-storey FIEB, the maximum storey drifts ratios stay by a large margin below the drift ratios estimated to produce a 10º rotation in the BIE's ends and bring these close to fracture.

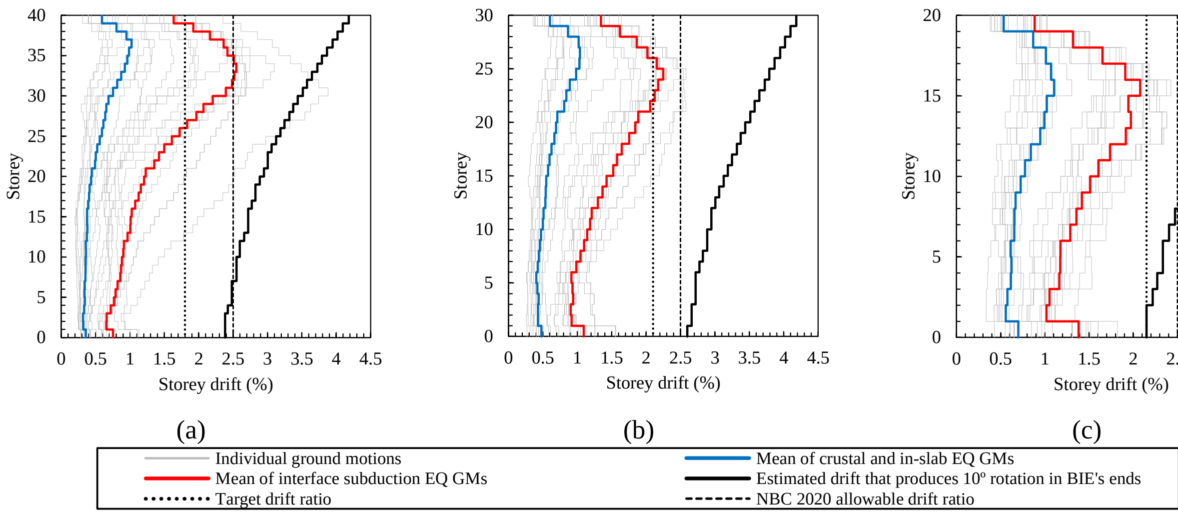

Figure 7. Maximum drift ratios for 40- (a), 30- (b), and 20-storey (c) FIEBs.

The residual drift ratios present in the buildings once the ground motions come to an end are shown in Figure 8. The observed average values are very low in comparison with the maximum drift ratios and remain well below 0.5%, indicating relatively low and presumably repairable damage [13]. Except for the storeys where the largest maximum storey drifts were observed in the 40-storey building, the average residual drifts for the crustal and in-slab subduction earthquake ground motions are of similar magnitude to those produced by the interface subduction earthquake ground motions, suggesting that the self-centering capability of BIEs is effective in contributing to restore the building close to its initial position.

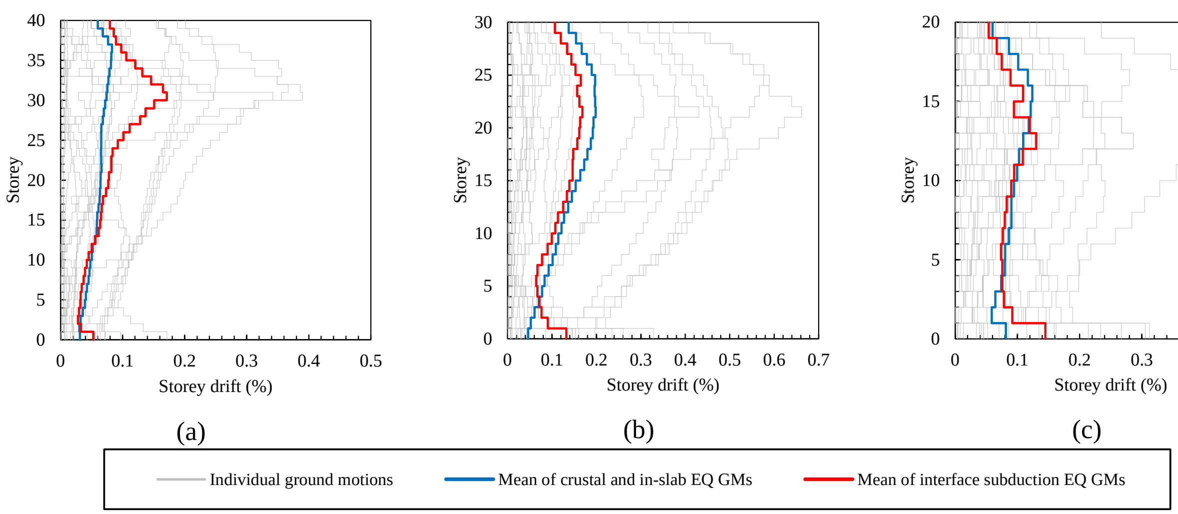

Figure 8. Residual drift ratios for 40- (a), 30- (b), and 20-storey (c) FIEBs.

The maximum storey shears developed by the BIEs in each storey are presented in Figure 9. These are calculated by summing the horizontal component of the axial force of the two opposed BIEs in each storey. Also shown are the capacity-based design shears, indicated by the thick black line, which are those employed in the design of the non-dissipating members of the SFRS. These were calculated as explained in [4] by assuming probable strength ($R_y F_y$) of the BIEs' material and that the maximum drifts would be 25% larger than the target drift at every storey. Overall, the maximum storey shears remain below the design shears, except for some slight overshoots in the case of the 40- and 30-storey buildings, attributed to the considerable higher mode effects and to incorporating materials with upper-bound yield strength values in the analyses.

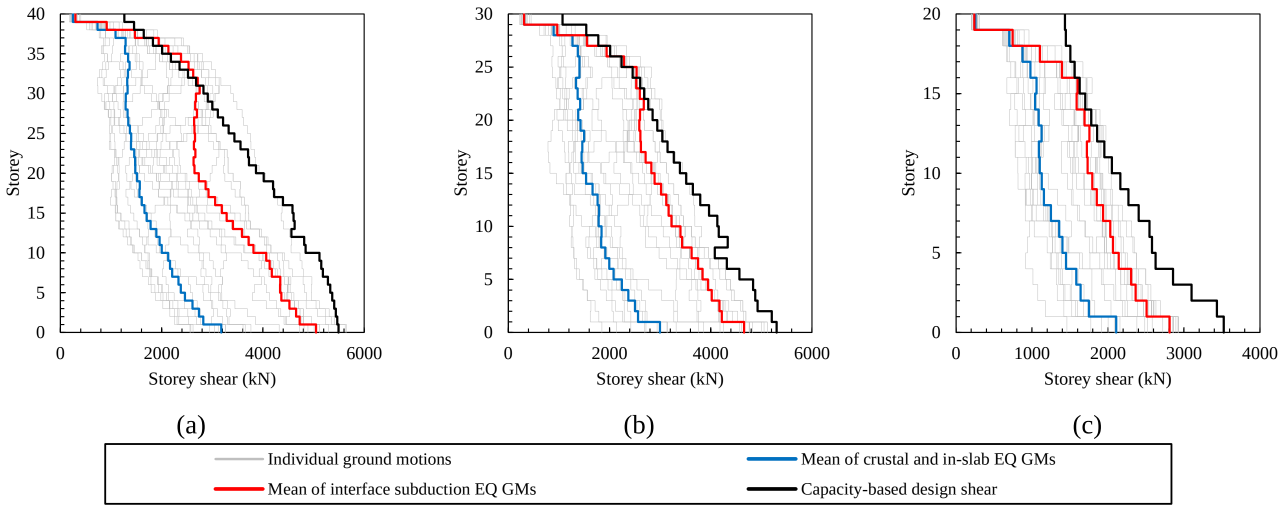

Figure 9. Maximum storey shears developed by BIEs for 40- (a), 30- (b), and 20-storey (c) FIEBs.

To verify how the energy dissipation was distributed over the buildings' height, stack plots of the energy dissipation histories by storey were plotted for the ground motions that produced the largest drift ratio demands. One of such plots is presented in Figure 10 for the interface subduction earthquake ground motion that produced the most severe demands, and the percentage of total dissipated energy by storey, for the same ground motion, is shown in Figure 11. Although for this example the first storey dissipated more energy than the rest, 6.5% of total, energy dissipation was fairly evenly distributed between storeys 2 to 32, with in average 2.9% of total each, before progressively reducing to zero toward the top of the building. Overall, the results show that in FIEBs, the smooth variation in storey stiffness and strength favoured an even engagement of the BIEs in plastic energy dissipation over the building height.

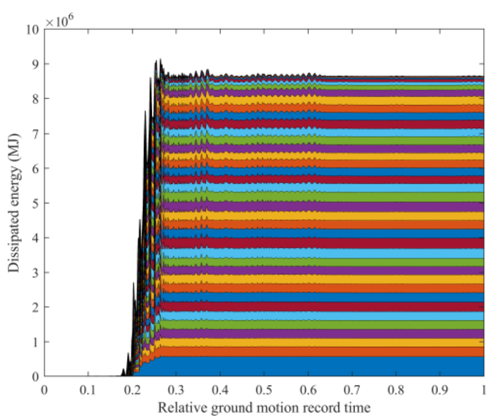

Figure 10. Stack plot of the energy dissipation history by storey for the interface subduction earthquake ground motion that produced the largest drift demands on the 40-storey FIEB.

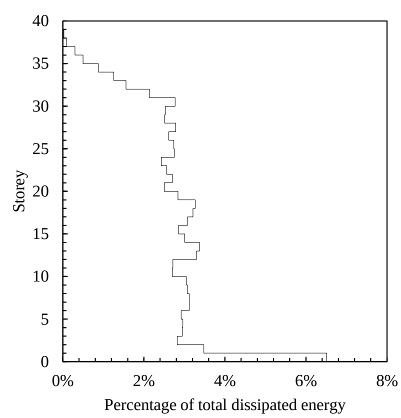

Figure 11. Energy dissipated by storey as percentage of total for the interface subduction earthquake ground motion that produced the largest drift demands on the 40-storey FIEB.

CONCLUSIONS

The suitability of FIEBs as the SFRSs of high-rise buildings was investigated by designing with a revised displacement-based procedure 20-, 30-, and 40-storey buildings located in a high seismic hazard region exposed to crustal, in-slab subduction, and interface subduction earthquakes, then assessing their performance through NLRHA.

The results show that the significant post-elastic stiffness of BIEs can be exploited to explicitly counteract the negative geometric stiffness associated with the P-Δ effects, thus ensuring adequate stability in the structure when subjected to long-duration ground motions. Additionally, the smooth variation in storey stiffness and strength over the building's height, enabled by the adjustment of the eccentricity, results in a better control of overstrength in comparison with traditional SFRSs and substantially reduces the possibility of a concentration of drift demands in an individual storey. Finally, the BIEs proved effective in producing moderate residual drift ratios, owing to their partial self-centering capability, of which the design procedure takes advantage.

Altogether, the results indicate that FIEBs possess the required attributes for their application as the SFRS of high-rise buildings such as those considered in this study. However, the overshoots in the predicted maximum storey drifts and storey shears, observed in particular for the 40-storey buildings, signal that the design procedure requires further revision to adequately incorporate higher mode effects, whose relative importance increase with building height. Also pending is the comparison of the performance and cost-effectiveness of FIEBs against those of SFRSs with well-established suitability for high-rise buildings.

ACKNOWLEDGMENTS

The first author acknowledges the Instituto Nacional de Investigaciones en Ingeniería (INII) and the Rectoría, both at Universidad de Costa Rica (UCR), for their support and financial assistance, respectively.

REFERENCES

[1] Skalomenos, K.A., Inamasu, H., Shimada, H., and Nakashima, M. (2017). "Development of a steel brace with intentional eccentricity and experimental validation". *Journal of Structural Engineering*, vol. 143, no.8, doi: 10.1061/(asce)st.1943-541x.0001809.

[2] González Ureña, A., Tremblay, R., and Rogers, C.A. (2022). "Experimental and numerical study of square HSS BIEs under cyclic loading". *Engineering Structures*, vol. 252, doi: 10.1016/j.engstruct.2021.113669.

[3] González Ureña, A., Tremblay, R., and Rogers, C.A. (2021). "Earthquake-resistant design of Frames with Intentionally-eccentric Braces". *Journal of Constructional Steel Research*, vol. 178, doi: 10.1016/j.jcsr.2020.106483.

[4] González Ureña, A., Tremblay, R., and Rogers, C.A. (2020). "Design and performance of Frames with Intentionally Eccentric Braces". In *17th World Conference on Earthquake Engineering*, Sendai, Japan.

[5] Skalomenos, K.A., Whitall, T., Kurata, M., and Pickering, J. (2022). "Component testing and multi-level seismic design of steel braces with high post-yielding stiffness and two-phase yielding". *Soil Dynamics and Earthquake Engineering*, vol. 157, doi: 10.1016/j.soildyn.2022.107248.

[6] Canadian Standards Association - CSA (2019). *CSA S16-19: Design of Steel Structures*. Prepared by the CSA, Toronto, ON, Canada.

[7] McKenna, F., Scott, M.H., and Fenves, G.L. (2010), "Nonlinear finite-element analysis software architecture using object composition". *Journal of Computing in Civil Engineering*, vol. 24, doi: 10.1061/ASCECP.1943-5487.0000002.

[8] Priestley, M.J.N., Calvi, G.M., and Kowalsky, M.J. (2007), *Displacement-based seismic design of structures*. IUSS Press, Pavia, Italy.

[9] González Ureña, A., Tremblay, R., and Rogers, C.A. (2020). "Numerical investigation of the seismic response of square HSS Braces with Intentional Eccentricity". In *17th World Conference on Earthquake Engineering*, Sendai, Japan.

[10] National Research Council of Canada – NRCC (2020). *National building code of Canada 2020*. Prepared by the NRCC, Ottawa, ON, Canada.

[11] National Research Council of Canada – NRCC (2017). *Structural commentaries (User's guide - NBC 2015: Part 4 of Division B)*. Prepared by the NRCC, Ottawa, ON, Canada.

[12] Halchuk, S., Adams, J., Kolaj, M., and Allen, T. (2019). "Deaggregation of NBCC 2015 seismic hazard for selected Canadian cities". In *12th Canadian Conference on Earthquake Engineering*, Québec, QC, Canada.

[13] McCormick, J., Aburano, H., Ikenaga, M., and Nakashima, M. (2008). "Permissible residual deformation levels for building structures considering both safety and human elements". In *14th World Conference on Earthquake Engineering*, Beijing, China.